Electronic Supplementary Material (ESI) for Nanoscale.

Supporting Information

Continuous ultrathin UiO-66-NH_2 coatings on polymeric substrate synthesized by layer-by-layer method: a kind of promising membranes for oil-water separation

Jian Gao, Wei Wei, Yuan Yin, Meihua Liu, Chunbai Zheng, Yifan Zhang * and Pengyang Deng*

1. Materials

$ZrCl_4$ (≥98.0%) and 2-aminoterephthalic acid (BDC-NH_2, ≥98.0%) were purchased from Alfa Aesar. Dimethylformamide (DMF) (A.R.), acetone (A.R.), C_2H_5OH (A.R.), potassium hydrogen phthalate (KHP, ≥99.8%) and phenolphthalein (A.R.) were purchased from Aladdin Industrial Corporation. Tetrahydrofuran (THF) (A.R.), KOH (A.R.), HCl (36%, A.R.) and NaOH (A.R.) were purchased from Beijing Chemical Works. Deionized water was used throughout all experiments. Nitrogen gas (≥99.999%) was purchased from Changchun JuYang company.

The substrates used in this work were purchased from commercial sources and include polymeric thin films made of polypropylene (PP) with a thickness of 0.05 mm and a mass density of 45 g/m^2; and non-woven fabric (NWF) made of PP with a thickness of 0.42 mm and a mass density of 120 g/m^2.

All substrates were washed with acetone and dried at 60°C for 3 h in a vacuum oven before use.

All reagents and materials in this work were used as received without further treatment.

2. Methods

(1) Attenuated total reflectance-Fourier transform infrared (ATR-FTIR) spectroscopy

Attenuated total reflectance-Fourier transform infrared (ATR-FTIR) analysis was performed on a Bruker Vertex 70 FTIR spectrometer equipped with an ATR unit (ATR crystal, 45°) at a resolution of 4 cm^{-1} for 32 scans. The samples (both powder and film) were used for measurement after activation at 120°C under vacuum overnight.

(2) X-ray diffraction (XRD)

X-ray diffraction (XRD) was performed on a Bruker D8 Advance diffractometer with a Cu-Kα X-ray radiation source (λ = 0.154056 nm). A scan rate of 0.02°/step and a scan time of 3 s/step over a 2θ range of 5~50° was used. Powder samples (ca. 20 mg) and film samples (cut into 40 × 40 mm sizes) were used for measurement after activation at 120°C under vacuum overnight.

(3) Field emission scanning electron microscopy (ESEM)

Field emission scanning electron microscopy (ESEM, XL-30) was applied to investigate the morphology of the samples. The SEM samples were preliminarily sputter-coated with gold.

(4) Energy-dispersive spectroscopy (EDS)

Energy-dispersive spectroscopy (EDS, Oxford X-MaxN 150), combining an SEM with EDS capability, was used to identify and quantify the elemental composition of the materials investigated in this work. When needed, samples were preliminarily sputter-coated with gold, except for analytical samples for the layer-by-layer (LBL) method.

(5) X-ray photoelectron spectroscopy (XPS)

X-ray photoelectron spectroscopy (XPS) data were obtained using a Thermo ESCALAB 250 electron spectrometer (Thermo Fisher Scientific) with an Al/K (hν =1486.6 eV) anode mono-X-ray source. The film samples (20 × 20 mm) were used for measurement after activation at 120°C under vacuum overnight.

(6) Measurement of surface carboxyl density (LRGs)

Quantitative measurement of the amount of carboxyl groups on the irradiation-grafted surfaces was conducted using NaOH-KHP titration according to the following process:

(i) Solution preparation

Preparation of 1 mM standard KHP solution: A total of 0.2042 g KHP was weighed after heated at 110°C for 2 h to remove water. Then, the KHP was transferred to a 1 L volumetric flask, deionized water was added, the flask was shaken, magnet was added, and the solution was stirred overnight at room temperature before use.

Preparation of ca. 1 mM NaOH solution: Approximately 0.040 g NaOH was weighed and transferred to a bottle, approximately 1 L deionized water was added, and the bottle was shaken. This solution was used immediately.

Preparation indicator solution: A total of 1.00 g phenolphthalein was weighed and transferred to a brown bottle, 100 ml ethanol was added, and the bottle was shaken well.

(ii) Sample processing

A total of 100 ml of NaOH solution (c.a. 1 mM) was added to a vial containing a irradiation-grafted substrate (~50 × 150 mm). The vial was then sealed and heated at 80°C for 2 h. A reference sample was also prepared.

(iii) Titration process

After cooling the vial, 20 ml of solution was removed from both the test sample and the reference sample, and 1 drop of indicator solution was added. The above solution was titrated using standard KHP solution (1 mM) until the pink colour disappeared.

The titration of each sample was repeated 3 times, and the titration volume of standard KHP solution used for each sample was averaged from the 3 tests.

(iv) Estimation of surface density of carboxyl groups (equal to crystal nucleus)

The surface density of carboxyl groups ($\rho_{-COOH,}$ nmol/cm^2) was estimated by the following equation:

$$\rho_{-COOH} = \frac{C_{KHP} \times (V_{ref} - V_t)}{S_{substrate}} \times 5 \times 1000 \quad (1)$$

where C_{KHP} (mmol/L) is the concentration of KHP solution, as prepared; V_{ref} (ml) is the titration volume of standard KHP solution for the reference sample; V_t (ml) is the titration volume of standard KHP solution for the test sample; $S_{substrate}$ (cm^2) is the substrate surface area (double-sided for films); *5* is the ratio of the total volume of NaOH solution (100 ml) to the volume of titrated NaOH solution (20 ml); and *1000* is the conversion factor from mmol to nmol.

(7) Contact angle

Contact angle goniometer (DSA30, Kruss, Germany) was used to measure the surface wettability of the sample. The contact angle of 5 positions was measured for each sample and averaged. The volume of liquid (water, silicone oil, soybean oil and petroleum ether) droplets was fixed to 2 μL during each measurement.

3. Results and discussion

3.1 Characterized of MAH-modified carboxyl polymer surfaces by co-irradiation grafting

The PP-g-MAH (or NWF-g-MAH) film was characterized by XPS. Untreated PP and NWF were also analysed for comparison, as shown in Figure S1 and Table S1. The change of carbon and oxygen content demonstrating that MAH was successfully grafted onto the surface (PP and NWF).

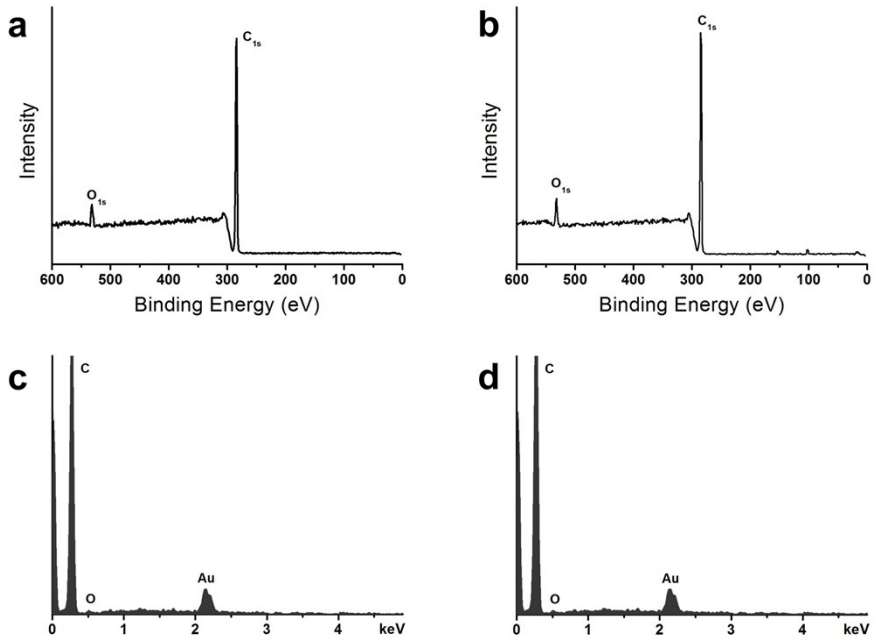

Figure S1. XPS and EDS spectrum of polymer substrate after grafted, (a) XPS of PP-g-MAH, (b) XPS of NWF-g-MAH, (c) EDS of PP-g-MAH, (d) EDS of NWF-g-MAH.

Table S1. Elemental composition of NWF and NWF-g-MAH surfaces, as determined from XPS survey spectra.

Sample	XPS Contents (at.%)		EDS contents (wt %)	
	C_{1s}	O_{1s}	C	O
PP	97.84	2.62	99.05	0.95
PP-g-MAH	96.15	3.85	98.66	1.34
NWF	97.16	2.84	98.75	1.25
NWF-g-MAH	94.17	5.83	98.13	1.87

3.2 Growing NTMCs on NWF-g-MAH by the LBL method

The preparation process of NTMCs on NWF-g-MAH (the surface density of grafted LRGs is 27.54 nmol/cm^2) was similar as that of NTMCs on PP substrate. Figure S2 shows large size UiO-66-NH_2@NWF-g-MAH prepared by LBL method. And the NTMCs was characterized by FTIR and XRD, as Figure S3 showed.

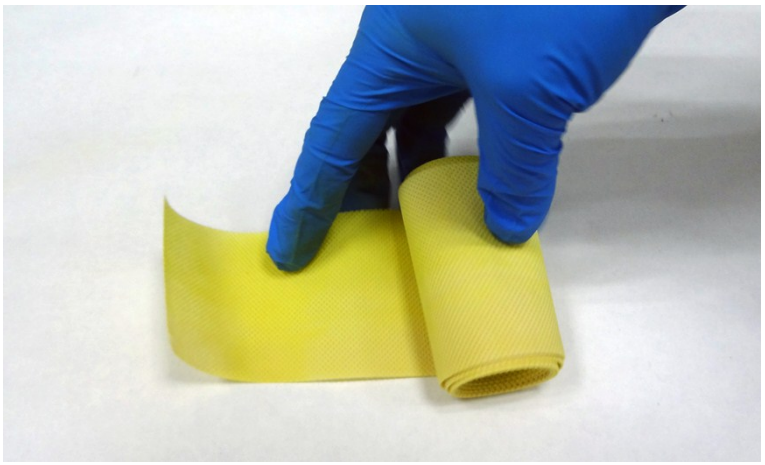

Figure S2. Photo of NTMC based on NWF-g-MAH prepared by LBL.

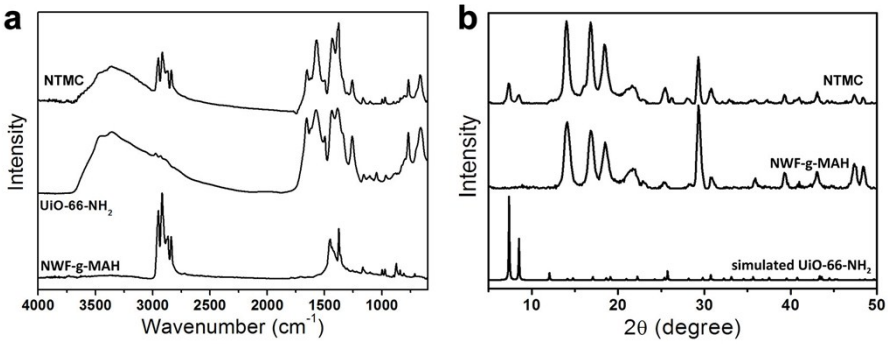

Figure S3. The characterization of NTMC on NWF prepared by LBL. (a) ATR-FTIR spectrum, (b) XRD pattern.

The morphology of NTMCs with different LBL cycles were was characterized by SEM, the sequential changes in the topological and geometrical properties of MOF coatings grown on NWF-g-MAH by the LBL process are shown in the SEM images in Figure S4. (1) LBL-1: no observable change in the surface morphology of fibres is noted, although the glossy surface of untreated PP-NWF fibres has been replaced by an opaque dense array of Secondary Building Units (SBUs), $Zr_6O_4(OH)_4$, at each surface-grafted –COOH; (2) LBL-2: no discernible features are yet observed on the surface, which now comprises the earlier array of SBUs with attached BDC-NH_2 organic ligands; and (3) LBL-3: the surface is uniformly covered by a monolayer homogeneous MOF coating with an average thickness of 85.5 nm (see Table S2) and average particle size of 167.3 nm. With subsequent repetition of steps (1) and (2), the particle size and coating thickness were further increased, as listed in Table S2. For these NTMCs, the particle size and the coating thickness continue to increase synchronously, and after the particle size reaches a plateau, the increase in coating thickness also slows down. The above analysis of the growth process of UiO-66-NH_2 coating on NWF further confirms the mechanisms observed during the LBL formation of UiO-66-NH_2@PP-g-MAH.

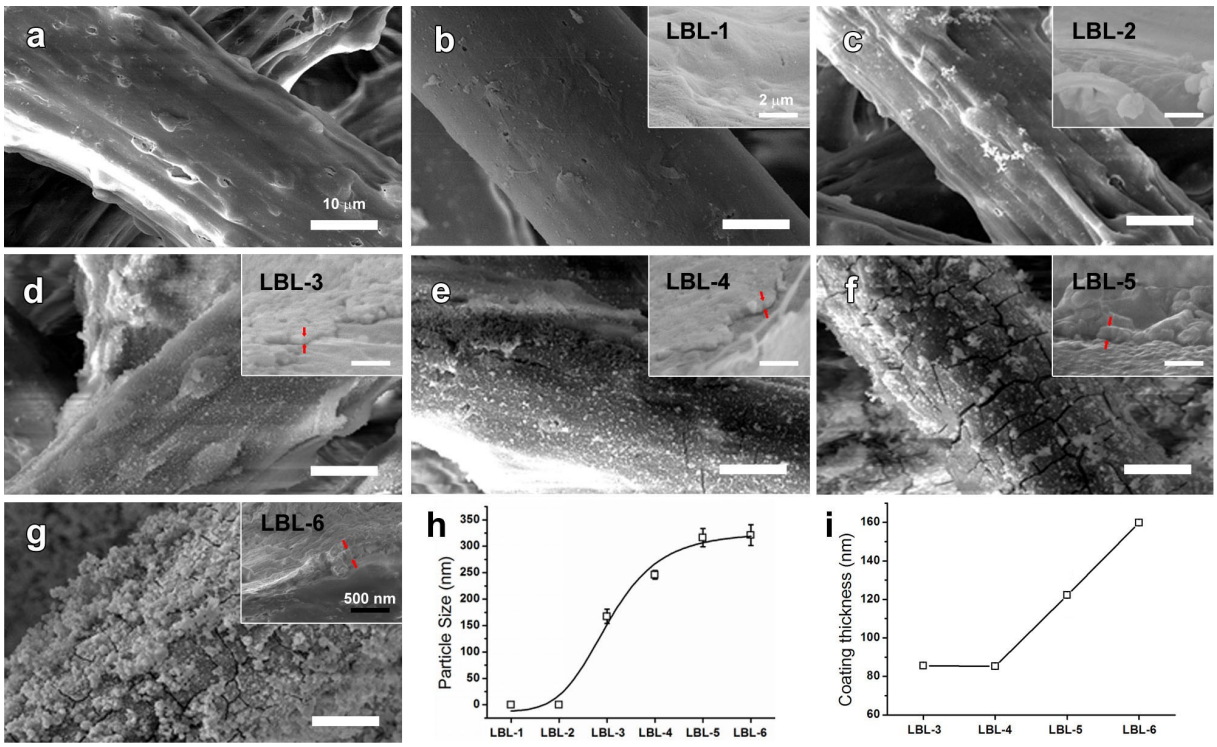

Figure S4. (a-g) SEM images of LBL-0, LBL-1, LBL-2, LBL-3, LBL-4, LBL-5 and LBL-6. The scale bar is 10 μm. The insets are cross-sectional SEM images of different NTMCs. The scale bars in the main panels, with the exception of (a), are 2 μm, whilst those in the insets are 500 nm. The red arrows mark thickness measurement positions. **(h)** Particle size at consecutive stages of the LBL process, **(i)** NTMC coating thickness at consecutive stages of the LBL process.

Table S2. Particle size and coating thickness of MOF coatings on NWF at consecutive stages of the LBL process, as obtained from SEM.

Sample	Particle size (nm)	Coating thickness (nm)
LBL-1	0	0
LBL-2	0	0
LBL-3	167.3	85.5
LBL-4	245.8	85.25
LBL-5	360.8	122.17
LBL-6	362.4	159.82

3.3 The thickness of MOF film based on PP substrate and NWF substrate

The cross-section of SEM of MOF film based on PP film (brittle fracture) and NWF (cut with knife) have been shown in the Figure S5, the thickness of MOF film based on PP is ca. 40 μm (marked on the image), and the thickness of MOF film based on NWF is ca. 58 μm (red marked, hot pressing) and 205 μm (blue marked).

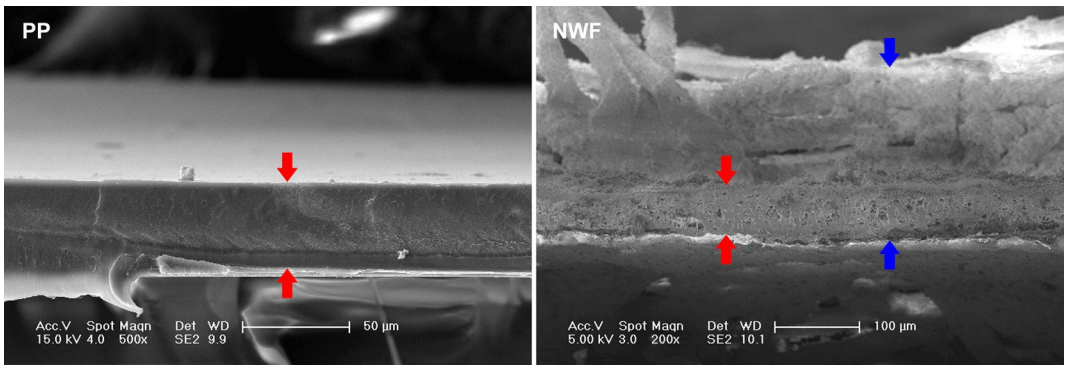

Figure S5. The cross-section SEM images of MOF films based on PP film and NWF.

3.4 Permeation experiment

To investigate the permeation ability of water and oil through NTMCs, a simple home-made liquid permeation device was used: NTMC (LBL-6, water contact angle 132.06° and the silicone oil contact angle is ~0°, UiO-66-NH_2@NWF-g-MAH) was cut into a circle with diameter of 21 mm and put into a screw cap, as Figure 7a showed. A simple filter of NTMC was obtained after screw the cap in a glass bottle which the bottom was removed, and such device was put on another bottle for liquid permeation (Fig. 7b and 7c). The permeation process of water (10 g) and soybean oil (10 g) through NTMC was showed in Video S1 and S2. The permeation rate for soybean oil is about 2 seconds per drop.

Unmodified NWF was used as comparison. Both water and soybean oil could permeate through unmodified NWF fast, as well as the oil-water mixture (shown in Figure S6), indicating that unmodified NWF could not be used for oil-water separation.

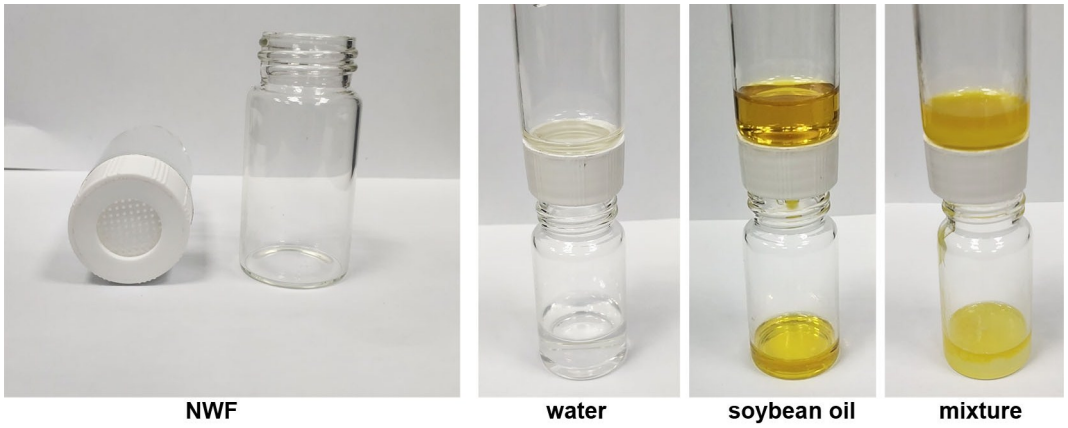

Figure S6. Photos of permeation result for NWF substrate.

3.5 The oil-water separation rate of NTMC

To further investigate the oil-water separation performance of NTMC, the oil-water separation rate of NTMC was caclulated by measuring the water content in the filtrate after oil-water separation (the mass ratio of oil/water is 1:1 before separation). And the water content was determined by Karl Fischer moisture titrator.

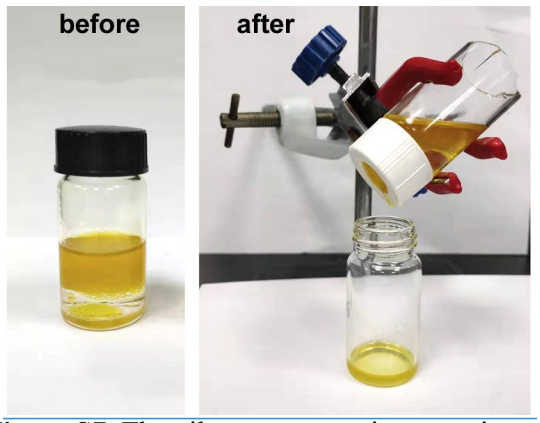

Figure S7. The oil-water separation experiment.

The oil-water separation rate of NTMC is 96.97%, which was listed in Table S3 and compared with the separation rate of other different separation membranes/films. Compared to different oil-water separation membranes/films, the oil/water separation performance of NTMC was good.

Moreover, NTMC is suitable for practical application which could be large-size prepared on different kinds of substrates. We believe the oil-water separation performance of NTMC will be further improved by optimizing the substrates.

Table S3. The oil-water separation rate of different oil-water separation membranes/films.

Sample	Substrate	Separation Rate	Ref
$Mg(OH)_2$	phenol-formaldehyde	92%	1
APT	PU	94-97%	2
TiO_2	porous Ti membrane	94.7-98%	3
ZnO	stainless steel mesh	95%	4
PDA-Ag	copper foams	95%	5
waste potato residue	stainless steel mesh	96.5%	6
PDA/cellulose	polyamide meshes	92-99%	7
PDMS	copper foam	98%	8
NTMC	PP non-woven fabrics	96.97%	This work

4. Reference

1 W. T. Cao, Y. J. Liu, M. G. Ma, et al. *Colloids and Surfaces A: Physicochemical and Engineering Aspects*, 2017, **529**, 18-25.

2 J. Li, L. Yan, H. Li, et al. *Rsc Advances*, 2015, **5**, 53802-53808.

3 L. Li, Z. Liu, Q. Zhang, et al. *Journal of Materials Chemistry A*, 2015, **3**, 1279-1286.

4 D. Tian, X. Zhang, Y. Tian, et al. *Journal of Materials Chemistry*, 2012, **22**, 19652-19657.

5 W. Zhou, G. Li, L. Wang, et al. *Applied Surface Science*, 2017, **413**, 140-148.

6 J. Li, D. Li, Y. Yang, et al. *Green Chemistry*, 2016, **18**, 541-549.

7 P. Zhao, N. Qin, C. L. Ren, et al. *Applied Surface Science*, 2019, **481**, 883-891.

8 X. Gao, J. Zhou, R. Du, et al. *Advanced Materials*, 2016, **28**, 168-173.